Published in Symposium Gyro Technology, 4.0-4.9, 1997
which should be used for any reference to this work

Error Modelling of a Silicon Angular Rate Sensor

C. Marselli, H.P. Amann and F. Pellandini
F. Grétillat, M.-A. Grétillat and N.F. de Rooij

Institute of Microtechnology, University of Neuchâtel
Rue A.-L. Breguet 2, CH 2000 Neuchâtel, Switzerland

http://www-imt.unine.ch

Abstract

The coupling between microsensors and efficient signal processing is essential to achieve demanding specifications for navigation applications. The performances of a silicon micromachined angular rate sensor are outlined showing that the main shortcoming consists of an important offset drift. This error is modelled and used in a correction algorithm based on Kalman filtering. The filter aims at estimating the sensor errors, like the offset, and the real angular rate, measuring the output voltage. Tests show that the accuracy is greatly improved.

1. Introduction

Advanced vehicle location systems will incorporate both a GPS (Global Positioning System) receiver and inertial sensors [1]. A signal processing system has to be investigated to maintain the accuracy of the navigation platform. The integration system must particularly estimate the inertial sensors errors due to external causes (e.g. temperature, pressure) as well as internal causes (e.g. parasitic vibration modes).

In this paper, the modelling of the bias error of a tuning fork silicon gyroscope (angular rate sensor) is presented [2]. This model is integrated in an error correction system based on Kalman filtering techniques [3].

In this project, both the sensor with its electronics and the navigation data processing are developed concurrently to achieve better efficiency and to take full advantage of this interaction.

2. Gyroscope Principle

The angular rate sensor is based on the tuning fork principle. It is operated by vibrating two tines anti-phase in one plane and measuring the effect of the Coriolis force in the orthogonal plane [2]. The tines are constructed from two proof masses suspended by four beams (Fig. 2.1).

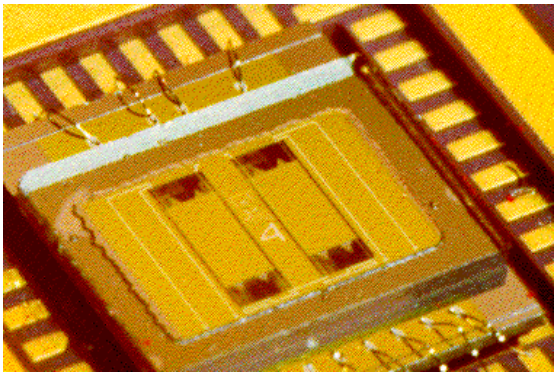

Fig. 2.1 : Picture of a packaged gyroscope. The two proof masses are 2000 µm long, 1000 µm wide and 360 µm thick.

Figure 2.2 illustrates the excitation principle of this sensor as well as its detection principle. A constant magnetic field (B) is provided by a magnet placed on top of the device. When an AC current flows along the

metallic conductor placed on top of the proof masses, the u-shaped design of this line results in an anti-phase Lorentz force. When rotating the gyroscope, the vertical movement of the proof masses due to the Coriolis force is sensed by means of four piezoresistors centred on top of the external suspensions and connected in a Wheatstone bridge configuration.

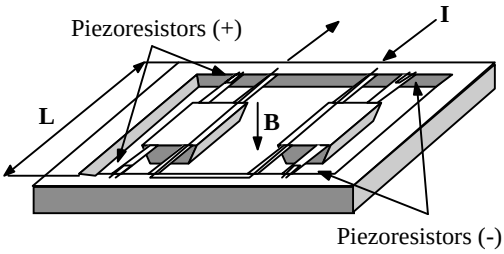

Fig. 2.2 : Top view of the gyroscope with the electromagnetic excitation and the piezoresistive detection.

3. Measurement set-up

To perform the dynamic measurements, the gyroscope output voltage has to be amplified 500 times to enable easy read-out. Then it is filtered by a lock-in amplifier as illustrated in Figure 3.1.

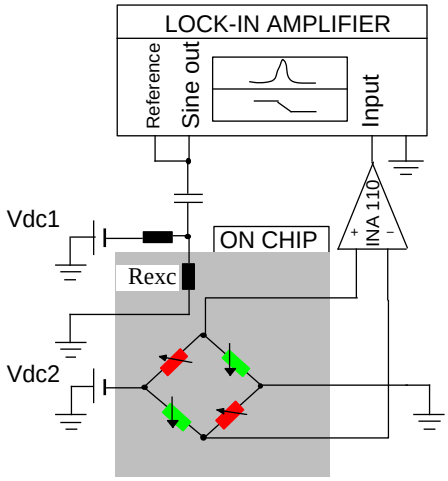

Fig. 3.1 : Experimental set-up for the dynamic measurements.

In view of the rotation measurements, the frequency of the driving current has to be fixed. Thus a frequency sweep without rotation is performed first. Figure 3.2 shows the voltage output of a (2000 µm x 1000 µm x 360 µm) prototype gyroscope.

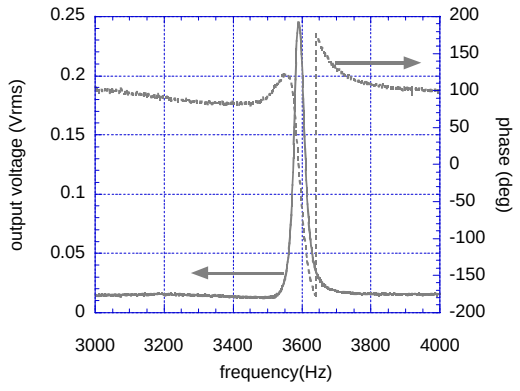

Fig. 3.2 : Frequency response with an AC excitation voltage of 1 Vrms.

Then the angular rate sensor with the electronic board is fixed on a rotating table (ACUTRONIC AG simple axis position rate table 120). Figure 3.3

illustrates the angular rate sensor output for two rates : 500 deg/sec clockwise (cw) and counter clockwise (ccw).

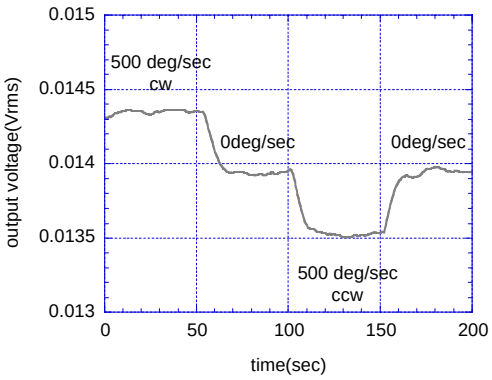

Fig. 3.3 : Output signal of a (2000 µm x 1000 µm x 360 µm) prototype gyroscope for several rotation rates.

By applying several rotation rates between ± 500 deg/sec, a sensitivity of 0.88 µm V/degsec^{-1} has been calculated by averaging the output voltage during 50 seconds neglecting the zero drift of the angular rate sensor (Fig. 3.4).

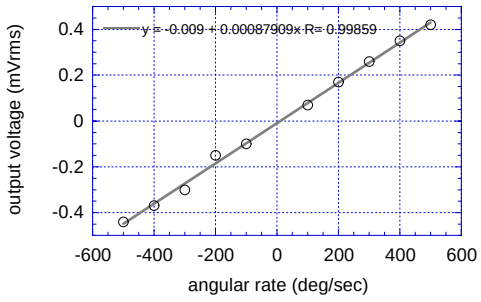

Fig. 3.4 : Output signal of a gyroscope prototype at different angular rates. The size of the proof masses is 2000 µm long, 1000 µm wide and 360 µm thick.

The lock-in amplifier, whose gain is 40 dB, is connected to a DSP (digital signal processor) board plugged in a PC host. Figure 3.5 shows the experimental set-up for long term measurements, which are needed for the offset characterisation.

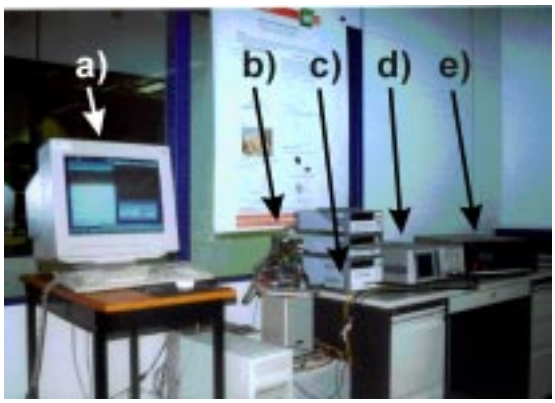

Fig. 3.5 : View of the experimental set-up with: a) the computer with the DSP card, b) the rotating table with the sensor in a metallic box, c) the power supply, d) the lock-in amplifier and e) the controller for the rate bench.

4. Modelling process

The Kalman filter [e.g. 5] requires a model of the system to be estimated. The search of models involves three basic steps. First, an experiment has to be designed to collect data from the process to be identified. Second, a model structure has to be chosen. Finally, the parameters of the model have to be estimated, guided by the data, using identification techniques. These three stages are detailed in the following.

4.1 Data record

The recording of the data is done using a DSP card (Texas Instruments TMS320C32). It includes a 16 bit A/D converter. The maximum range of the input signal is ± 3V, leading to a resolution of 0.18 mV.

Since the input filter of the DSP card has a minimum cut-off frequency of 600 Hz, the sampling frequency has been set to 1280 Hz to avoid aliasing. During file recording, the signals are decimated (rate 1/5) after suitable low-pass filtering. Finally, they are resampled again from 256 Hz to 32 Hz with an off-line processing. The suitable bandwidth for navigation needs is indeed in a ten Hz range.

There is no absolute rule to set the duration of acquisition. It just must be long relative to the typical variations of the signals. Otherwise, attempts to characterise the spectral contents would fail. For this case, the gyro output has then been recorded during several minutes (about 10 mn) to characterise its offset.

4.2 Model structure

As the offset varies in a random manner, an ARMA (autoregressive moving average) model is used. Since the models are put in a Kalman filter, the state space form of an ARMA signal is also given.

4.2.1 ARMA model

An ARMA signal y(k) is defined as the output of a linear dynamic system having a rational transfer function with n poles a_i (i=1:n) and m zeros b_j (j=1:m) and submitted to white noise e(k) as input :

$$y(k) + a_1 y(k-1) + \cdots + a_n y(k-n) = b_0 e(k) + b_1 e(k-1) + \cdots + b_m e(k-m)$$

Because of the poles and zeros, the flat spectrum of the white noise is modified to fit the spectrum of the random process to be identified.

4.2.2 ARMA signal state-space form

The state space form of a system is :

$$X_{k+1} = A_k X_k + G_k w_k$$

$$y_k = C_k X_k + L_k v_k$$

where X_k is the state vector, y_k is the measurement of the system, w_k and v_k are white noises. A_k, G_k, C_k, L_k are link matrices. The chosen expression of an ARMA signal in such a form leads to :

state matrix

$$A_k = \begin{bmatrix} -a_1 & 1 & 0 & \cdots & \cdots & \cdots & 0 \\ -a_2 & 0 & 1 & 0 & \cdots & \cdots & 0 \\ -a_3 & 0 & 0 & 1 & 0 & \cdots & 0 \\ \vdots & \vdots & \ddots & \ddots & \ddots & \ddots & \vdots \\ \vdots & \vdots & \ddots & \ddots & \ddots & \ddots & 1 \\ -a_n & 0 & \cdots & \cdots & \cdots & \cdots & 0 \end{bmatrix}$$

observation matrix

$$C_k = [1 \quad 0 \quad 0 \quad \cdots \quad \cdots \quad \cdots \quad 0]$$

state noise coupling matrix

$$G_k = \begin{bmatrix} b_1 - b_0 a_1 \\ b_2 - b_0 a_2 \\ \vdots \\ b_m - b_0 a_m \\ -b_0 a_{m+1} \\ \vdots \\ -b_0 a_n \end{bmatrix}$$

measurement noise coupling matrix

$$L_k = b_0$$

4.3 Identification method

The identification stage is done with the help of the *System Identification Toolbox* of *Matlab*^{TM}. It provides a collection of model structures and estimation techniques. In the following, the parameters of the ARMA model are identified using an iterative Gauss-Newton algorithm [4].

5. Kalman filter design

5.1 Motivation

The algorithm used to correct the sensor errors like the offset is based on a Kalman filter. Before giving its derivation, its design is justified below.

Kalman filtering has been used extensively in navigation applications since the mid 60' and more recently in the integration of GPS with inertial sensors [6], where the complementary filter approach is used. In such applications, redundant measurements of the same information are available, and the filter has to combine all data in such a way as to minimise the instrumentation errors. More exactly, the state vector contains the position and velocity computed with the inertial system as well as the sensor errors. The observation vector contains the aiding sources. A similar filter has been designed for the whole project, in which this research takes place and which is related to the realisation of a navigation microsystem. It has been studied for a reduced set of sensors suitable for automotive navigation (3 sensors instead of the 6 usually recommended). However the derivation of the filter equations is not the main purpose of this paper and is not given here. In these classical algorithms, the angular rate is directly put in the Kalman filter. The underlying assumption is that the calibration parameters (scale factor and offset) given by the manufacturer are precise. This is not realistic for microsensors, which are further less accurate than mechanical ones. Therefore, it can be worthwhile to estimate the calibration parameters. Here, another Kalman filter is proposed. For this case, the state vector contains offset, sensitivity

and angular rate. The observation does not come from an external source but from the sensor output voltage. The voltage depends on the real angular rate and the sensor errors.

Finally, let us mention a major difference between the two approaches. Since aiding sources data arise less often than the inertial information, the complementary filter relies above all on the state models without taking benefit of the observation model. On the contrary, the rate of prediction and update stages is equal in the proposed filter, because the voltage is continuously available.

5.2 Derivation of equations

The gyro output voltage is related to the angular rate by :

$$U_g = (k_o + k_g)\omega + o_g$$

where k_o is the nominal scale factor given by the manufacturer, k_g is the scale factor variation, ω is the angular rate which is applied to the gyro, and o_g is the offset variation.

The state vector contains the sensitivity and offset variations as well as the angular rate. Its length n depends on the number of variables needed to describe the models found in a state space form.

$$X_k = \begin{bmatrix} k_{g1} \\ \vdots \\ k_{gp} \\ o_1 \\ \vdots \\ o_{gq} \\ \omega \end{bmatrix}$$

The observation is simply the gyro output voltage. Since the relationship between the variables is non-linear, an extended filter is used. Therefore, the state matrix is :

$$A_k = \left.\frac{\partial f_k}{\partial x_k}\right|_{\hat{x}_k} \text{ where}$$

$$\omega = \frac{U - o_1}{k_o + k_1} = f(k_1, o_1)$$

The n-1 rows of the state matrix are the error model description. The last row is given by the partial derivatives of f regarding the state variables :

$$A(n,1) = \frac{\partial f(k_1, o_1)}{\partial k_1} = -\frac{U - o_1}{(k_0 + k_1)^2}$$

$$A(n,p+1) = \frac{\partial f(k_1, o_1)}{\partial o_1} = -\frac{1}{k_0 + k}$$

$$A(n,n) = \frac{\partial f(k_1, o_1)}{\partial \omega} = 0$$

Similarly, the observation matrix is :

$$C_k = \left.\frac{\partial h_k}{\partial x_k}\right|_{\hat{x}_{k(-)}} \text{ where}$$

$$U_g = (k_o + k_1)\omega + o_1 = h(k_1, o_1, \omega)$$

One has :

$$C(1) = \frac{\partial h(k_1, o_1, \omega)}{\partial k_1} = \omega$$

$$C(p+1) = \frac{\partial h(k_1, o_1, \omega)}{\partial o_1} = 1$$

$$C(n) = \frac{\partial h(k_1, o_1, \omega)}{\partial \omega} = k_o + k_1$$

5.3 Simulation results

The filter has been validated by simulations. In the following example, a simulated voltage is created as a sum of sinusoids added to an ARMA noise, whose model is known. Figure 5.1 shows that the filter succeeds in recovering the real angular rate.

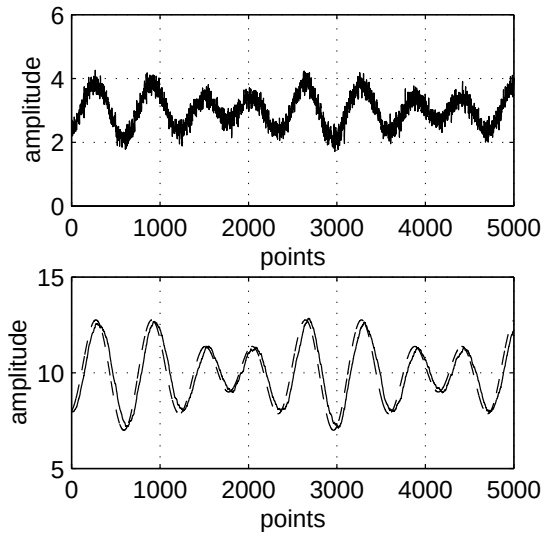

Fig. 5.1 : (top) Simulated output voltages - (bottom) Ideal angular rate (dotted line) and estimated one. The offset ARMA model is defined by 2 poles (a_1 =-1, a_2 = 0.5) and 1 zero (b_1 = 0.1). The sensitivity is set to 0.3.

6. Correction examples

The correction of the offset drift is presented below. The sensitivity is assumed to be constant. Its value is 0.88 μm V/degsec^{-1} (cf. §2).

6.1 Offset models

Figure 6.1 shows a typical measurement of the gyro output recorded over a period of 15 mn.

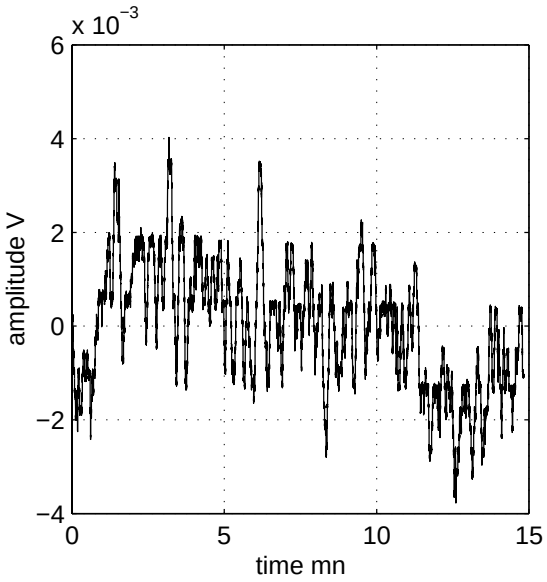

Fig. 6.1 : Offset measurement.

The offset model is thought as the addition of an ARMA noise and an integrator to taking into account the unbounded drift.

An ARMA signal having 4 poles and 3 zeros (Fig. 6.2) has been searched to fit the power spectral density (PSD) of the signal (Fig. 6.3). The frequency fitting of the model has been checked on several realisations of the signals.

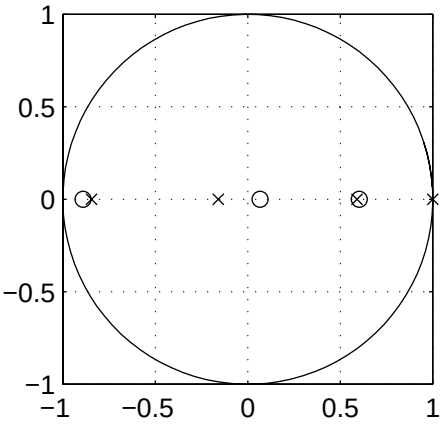

Fig. 6.2 : Poles and zeros given by the identification stage ‘o’ denoting zeros and ‘x’ poles.

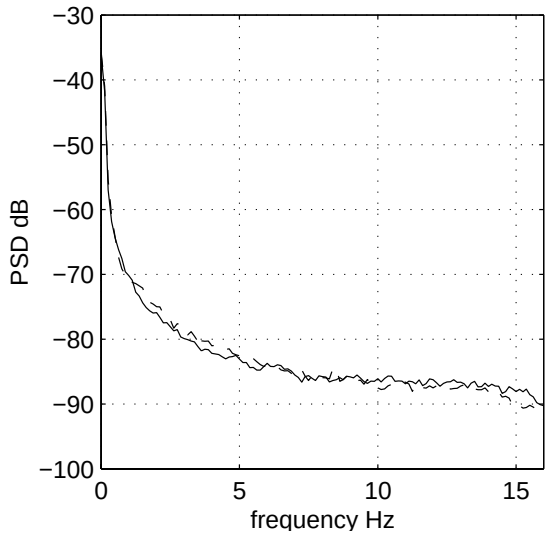

Fig. 6.3 : Comparison of the PSD of the model (solid line) and of the measurement (dotted line).

The drift is modelled by an integrator :

$$\begin{bmatrix} d_1 \\ d_2 \end{bmatrix}_{k+1} = \begin{bmatrix} 1 & 1 \\ 0 & 1 \end{bmatrix} \cdot \begin{bmatrix} d_1 \\ d_2 \end{bmatrix}_k + \begin{bmatrix} 0 \\ \sigma \end{bmatrix} w_k$$

d_2 is the slope of the drift and is expressed by a random constant, which is initialised regarding the measurements.

6.2 Improvements

Figure 6.4 shows the offset before and after correction. Two different corrections are illustrated where the R (measurement noise covariance matrix) factor has been changed. The more the R value is small, the more the filter is confident of the observation model. The value of Q is given by the ARMA model identification.

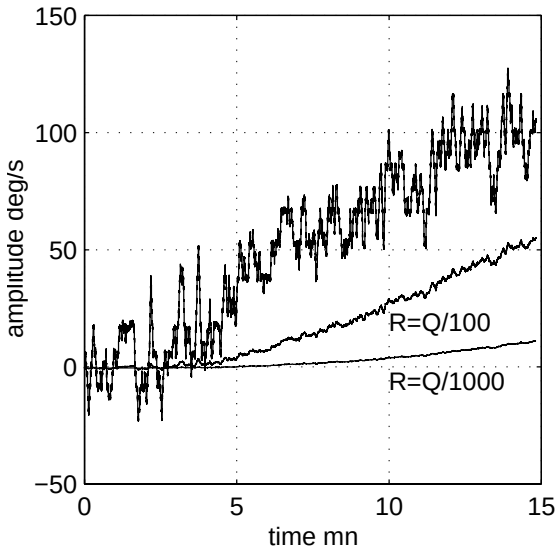

Fig. 6.4 : Correction of the offset.

6.3 Varying velocity tests

Figure 6.5 shows an experiment where the angular velocity is changed from 0 deg/s to 100 deg/s in the middle of the recording period. The correction algorithm, including the previously described model, allows to reduce the drift and to improve the accuracy.

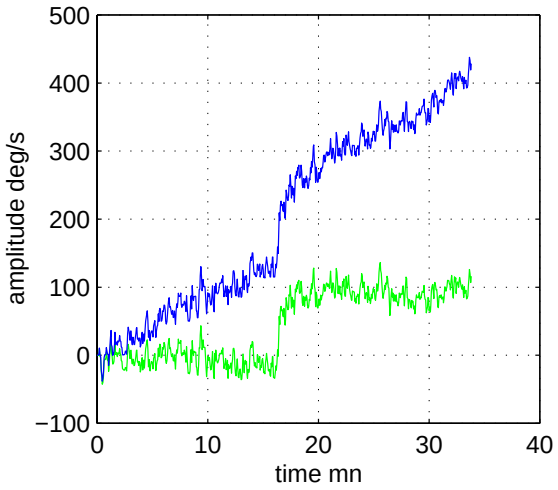

Fig. 6.5 : Step change of angular velocity : without (black) and with (grey) correction.

7. Conclusion

An algorithm based on Kalman filtering for correcting the offset drift of a micro machined angular rate sensor has been presented. It leads to great improvements. Future work includes tuning of the filter parameters and further modelling. In the same time, a new design of the sensor is being investigated. The predicted better performances combined with the signal processing algorithms aim at fulfilling the demanding specifications of navigation applications.

8. Acknowledgements

This work has been funded by the Swiss National Science foundation (FNSRS) and the Swiss Foundation for Research in Microtechnology (FSRM) in the frame of an international exchange between French and Swiss institutions active in the field of microtechnology (PICS : Projet International de Coopération Scientifique)

9. References

[1] J. Söderkvist, “Micromachined gyroscopes”, Sensors and Actuators A, vol. 43 (1994), pp. 65-71

[2] F. Paoletti, “A silicon micromachined tuning fork gyroscope”, Proc. of the Symposium Gyro Technology 1996, Stuttgart Germany, September 17-18 1996, pp. 5.0-5.8

[3] C. Marselli, “Error correction applied to microsensors in a navigation application”, 3rd France-Japan Congress, Besançon France, October 1-3 1996, pp. 650-655

[4] Ljung L., “System identification : Theory for the User”, Prentice Hall, 1987

[5] Grewal M., Andrews A., “Kalman filtering : theory and practice”, Prentice Hall Information, 1993

[6] R.V.C. Wong, K.P. Schwarz, “Dynamic Positioning with an integrated GPS-INS”, UCSE reports, University of Calgary, Alberta, Canada, 1985